

MARIOLA BUCZKOWSKA

Institute of Physics, Lodz University of Technology, ul. Wólczańska 219,
90-924 Łódź, Poland, e-mail: mariola.buczowska@p.lodz.pl

FLEXOELECTRO-OPTIC EFFECT WITH LARGE ROTATION ANGLE OF OPTIC AXIS

The flexoelectro-optic effect in layers of chiral nematics was investigated numerically. The simulations concerned short pitch materials with the helix axis parallel to the layer plane. Configurations which allow to avoid accumulation of ions at the electrodes and are suitable for square-wave driving voltage were considered. They were related to large rotation angles of the optical axis of the layer about the normal to the layer. Influence of chosen parameters on efficiency of the electro-optic effect was studied.

Keywords: chiral nematic, helical axis, flexoelectro-optic effect.

1. INTRODUCTION

The flexoelectro-optic effect occurs in layers of chiral nematic liquid crystals in which the helix axis is parallel to the layer plane due to homeotropic boundary conditions (Uniform Lying Helix (ULH) structure) [1-4]. The layer is placed between crossed polarisers. If the intrinsic pitch p_0 is shorter than the wavelength of visible light, the layer behaves as a plate of uniaxial birefringent medium. In the absence of external electric field, the effective optic axis coincides with the helix axis. Electric field of strength E , applied perpendicular to the layer by means of transparent electrodes deposited on the boundary plates, interacts with the flexoelectric polarization of the liquid crystal and induces director rotation about the normal to the layer. This effect is equivalent to in-plane rotation of the optic axis which is perpendicular to the twisted director. The rotation angle Φ is approximately proportional to the field strength giving fast linear electro-optic effect with sub-millisecond response times [5]. If the boundary conditions allow for variation of the pitch under the action of external field, the voltage dependence of the rotation angle is described by the formula

$$\tan\Phi = \frac{(e_{11} - e_{33})E}{(k_{11} + k_{33})q_0}, \quad (1)$$

where k_{ii} are the elastic constants, e_{ii} are the flexoelectric coefficients and $q_0 = 2\pi/p_0$. If the pitch cannot vary because of surface interactions, the rotation angle is given by [6-8]

$$\tan\Phi = \frac{(e_{11} - e_{33})E - (k_{11} + k_{33} - 2k_{22})q_0 \sin\Phi}{2k_{22}q_0}. \quad (2)$$

The direction of rotation depends on the sign of bias voltage. In the commonly considered configuration, the undistorted optic axis is oriented at the angle $\alpha = 22.5^\circ$ with respect to one of the polarisers [2,3]. The optical transmission T can be switched between 0 and 1 if the rotation angle Φ varies between $+22.5^\circ$ (obtained when $U = U_{max}$) and -22.5° (obtained when $U = -U_{max}$). A given value of transmission is due not only to the magnitude but also to the sign of the bias voltage. If some value of transmission is to be constant, the sign of the voltage should be maintained as well, therefore the ions accumulate at the electrodes which is undesirable [7].

In this paper, other configurations with large field induced rotation angle $|\Phi| = 45^\circ$ are considered. They offer the flexoelectro-optic effect that can be driven by square-wave voltage which ensures reduction of ions accumulation. Such flexoelectro-optic effect was presented in [9]. Very large rotation angles equal to $\pm 45^\circ$ are also needed in order to achieve a full 2π phase modulation range in flexoelectro-optic spatial light modulators [10]. The aim of this study is to show what values of parameters should be chosen in order to obtain the rotation angles as large as 45° by application of voltages as small as those sufficient for $|\Phi| = 22.5^\circ$. The corresponding assumptions are described in the next section. The results of numerical calculations are presented in Section 3 where the voltage dependences of Φ are determined for several sets of parameters.

2. ASSUMPTIONS AND METHOD

2.1. Optical transmission

The flexoelectro-optic effect free from accumulation of ions can be realised provided that several conditions are satisfied. In order to analyse the optical transmission of the system, the ULH layer can be treated as a plate of birefringent medium with electrically tunable optic axis placed between crossed

polarisers. The birefringence of liquid crystal, $\Delta n = n_e - n_o$, should be suitably chosen in order to satisfy the condition

$$\sin^2 \frac{\delta}{2} = 1 \quad (3)$$

which is necessary to obtain maximum transmission, where $\delta = 2\pi d\Delta n/\lambda$ is the phase difference between ordinary and extraordinary waves. Condition (3) is satisfied if $\delta = \pm\pi(2k-1)$, where $k = 1, 2, \dots$.

In the case of crossed polarisers, the optical transmission of the system is given by the general formula [11]

$$T_{\perp} = \sin^2 2\phi \sin^2 \frac{\delta}{2}, \quad (4)$$

where $\phi = \alpha + \Phi$ is the angle between one of the polariser and the optic axis rotated by Φ .

If $\alpha = 45^\circ$, the transmission in the absence of voltage (i.e. if $\Phi = 0^\circ$), reaches maximum, $T_{\perp} = 1$. The positive as well as negative bias voltages of the same absolute value, U and $-U$, induce rotation angles Φ and $-\Phi$ of the same magnitude. If Φ reaches 45° or -45° , the optical transmission drops to zero, $T_{\perp} = 0$.

If $\alpha = 0^\circ$, the transmission in the absence of voltage is zero. If the rotation angles induced by voltages U and $-U$ reach 45° or -45° , the optical transmission is maximum, $T_{\perp} = 1$.

In the case of parallel polarisers, the optical transmission of the system is given by [11]

$$T_{\parallel} = \left(1 - \sin^2 2\phi \sin^2 \frac{\delta}{2} \right). \quad (5)$$

If $\alpha = 45^\circ$ and $\Phi = 0^\circ$, the transmission is zero. The rotation angles Φ and $-\Phi$ give the same values of transmission, reaching $T_{\parallel} = 1$ if $|\Phi| = 45^\circ$.

If $\alpha = 0^\circ$ and $\Phi = 0^\circ$, the transmission is maximum, $T_{\parallel} = 1$, whereas it drops to zero if $|\Phi| = 45^\circ$.

The above considerations show under what circumstances the optical transmission of the system is independent of the sign of the applied voltage, as long as the magnitude of the voltage is maintained. This allows to drive the system by square-wave voltage which reduces the ionic polarization of electrodes.

2.2. Geometry and parameters

The chiral nematic liquid crystal layer of thickness d was taken into account. The layer was parallel to the xy plane of the coordinate system. It was placed between two transparent electrodes positioned at $z = \pm d/2$. The helical axis was directed along the y axis. Director orientation was determined by the polar angle $\theta(y,z)$ made between the director and its projection on the xy plane, and by the azimuthal angle $\phi(y,z)$ between this projection and the x axis. Both angles as well as all other quantities were independent of the x coordinate. The chirality of the nematic was determined by the intrinsic pitch, smaller than wavelength λ of visible light, $p_0 < 0.4 \mu\text{m}$. Homeotropic boundary conditions were assumed. The anchoring energy was determined by the polar and azimuthal anchoring strength coefficients, $W_\theta = 10^{-4}$ and $W_\phi = 10^{-5} \text{Jm}^{-2}$, respectively [12]. The layer was subjected to voltage U ranging from 0 to 35 V. Dielectric anisotropy was assumed to be zero or ± 5 V. Several sets of the system parameters were used during computations. They are mentioned in Table 1 and labelled with letters (a) - (j).

In order to obtain the rotation angle Φ as large as 45° the nematic material should possess special features. In particular, the strong flexoelectric properties are desirable. Significant flexoelectric properties are characteristic for bent core or bimesogenic nematics [13-15]. On the other hand, these substances exhibit unique ratios between elastic constants. We simulate such materials using the values $k_{11} = 7 \text{ pN}$, $k_{22} = 2 \text{ pN}$, $k_{33} = 7 \text{ pN}$. Typical elastic constants of calamitic nematic were also adopted for comparison: $k_{11} = 8 \text{ pN}$, $k_{22} = 4 \text{ pN}$, $k_{33} = 12 \text{ pN}$. Parameters in the sets (b) - (h) were chosen in order to illustrate the role of elastic constants, flexoelectric parameter $e_{11} - e_{33}$, intrinsic pitch p_0 and thickness d . It was assumed that the pitch was independent of bias voltage in all these cases.

The value of voltage which induces the rotation angle equal to 45° can be used as a characteristic of the efficiency of flexoelectro-optic effect. The values corresponding to all the parameters sets are mentioned in Table 1 denoted as U_{45} .

2.3. Method

The deformations of the director field inside the ULH layer were calculated by means of minimization of the free energy counted per unit area of the layer. For this purpose, we used the method which was successfully applied in earlier works [16]. The electric potential distribution $V(y,z)$ in the layer was calculated by resolving the Poisson equation.

Table 1

The sets of parameters used during computations

	k_{11}, k_{22}, k_{33} [pN]	$e_{11} - e_{33}$ [pC/m]	p_0 [nm]	d [μm]	$\Delta\varepsilon$	U_{45} [V]
(a)	7, 2, 7	20	300	2	0	23.02
(b)	7, 2, 4	20	300	2	0	18.53
(c)	7, 4, 7	20	300	2	0	25.38
(d)	7, 1, 7	20	300	2	0	21.91
(e)	7, 2, 7	40	300	2	0	11.62
(f)	7, 2, 7	20	250	2	0	27.65
(g)	7, 2, 7	20	300	3	0	34.46
(h)	8, 4, 12	20	300	2	0	34.22
(i)	7, 2, 7	20	300	2	5	27.22
(j)	7, 2, 7	20	300	2	-5	50.83

3. RESULTS AND CONCLUSIONS

The example of strong deformation of the ULH structure reaching $\Phi = 45^\circ$ is presented in Fig. 1 by means of cylinders symbolizing the director.

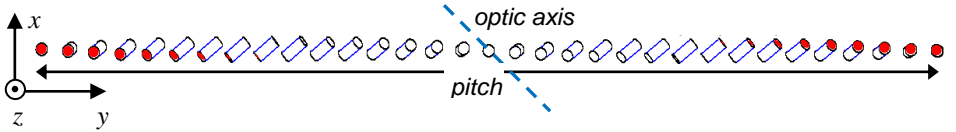


Fig. 1. Director distribution over the distance of single pitch as seen along the z axis; a single row located in the mid-plane of the layer is shown; parameters set (a); $U = 23$ V, $\Phi = 45^\circ$; the optic axis is also drawn.

For high efficiency, the absolute value of U_{45} should be as low as possible. Influence of parameters on the efficiency of the system is illustrated in Figs. 2 - 4. It is evident from curves (a) - (d) shown in Fig. 2 that low values of the sum of elastic constants $k_{11} + k_{33}$ and big values of k_{22} are preferable since they lower the magnitude of U_{45} as indicated by formula (2)

$$U_{45} = \frac{2\pi(k_{11} + k_{33})d}{(e_{11} - e_{33})p_0} \quad (6)$$

The elastic constants typical for calamitic nematics (curve (h)), give significantly higher value.

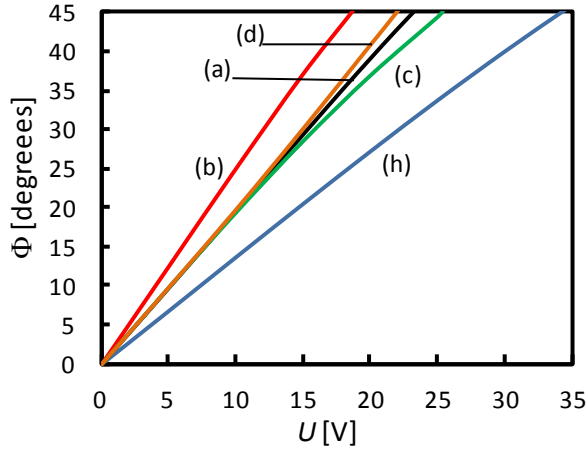


Fig. 2. Rotation angle Φ as a function of bias voltage. The curves (a), (b) (c) (d) and (h) correspond to sets of parameters mentioned in Table 1. Role of elastic constants is illustrated.

Fig. 3 shows that strong flexoelectric properties described by $e_{11} - e_{33}$, long intrinsic pitch p_0 and small layer thickness also lower the value of U_{45} .

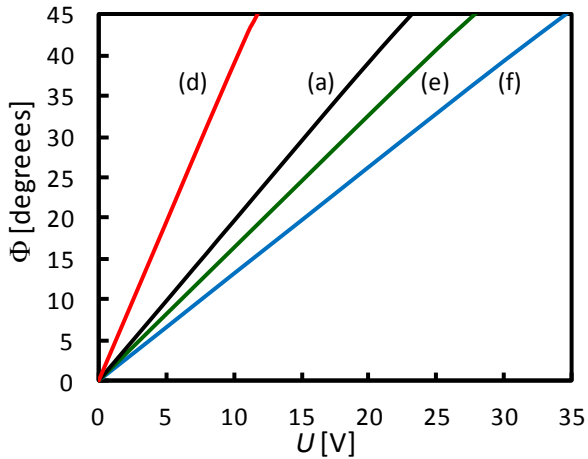


Fig. 3. Rotation angle Φ as a function of bias voltage. The curves (a), (e) (f) and (g) correspond to sets of parameters mentioned in Table 1. Role of flexoelectricity (e), pitch (f) and thickness (g) is illustrated.

The role of dielectric anisotropy was also investigated. Calculations performed with the parameters sets (i) and (j) revealed that the rotation angle varies along the y axis which can be described by the formula [17]

$$\Phi(y) = \Phi_0 + \Delta\Phi \cos(4\pi y/p_0), \quad (7)$$

where the mean value Φ_0 and the amplitude $\Delta\Phi$ depend on z in the vicinity of the boundaries only. The amplitudes $\Delta\Phi$ are rather small and do not exceed ten degrees (Fig. 4). The $\Phi_0(U)$ dependence deviates from proportionality. In our case, both positive and negative dielectric anisotropy lead to increase of U_{45} (in contrast to Ref. [18] where the negative anisotropy lowered the value of U_{45} .)

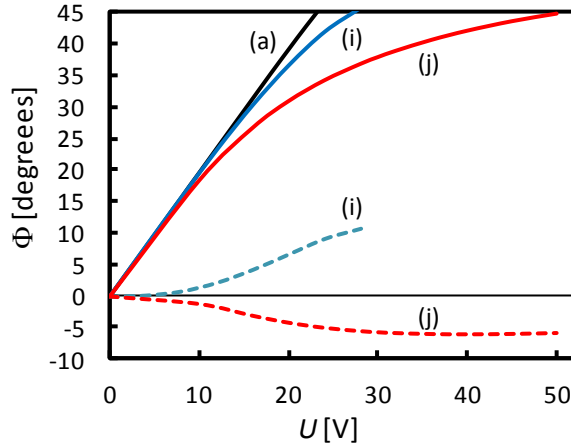


Fig. 4. Voltage dependences of mean rotation angle Φ (full line) and amplitude $\Delta\Phi$ (dashed line). The curves (a), (i) and (j) correspond to sets of parameters mentioned in Table 1. Role of dielectric anisotropy is illustrated.

Additional calculations showed that if the pitch is not maintained by the surface interactions and it shortens under the action of the field [6] according to formula $p = p_0 \cos\Phi$, then the voltage U_{45} becomes significantly higher (Fig. 5).

In conclusion, the flexoelectro-optic effect can be driven by square wave voltage if the rotation angle reaches 45° . Such large angle requires application of voltage of significant magnitude. From practical point of view the amplitude of bias voltage should be as low as possible. Therefore the values of the system parameters should be suitable chosen. Optimally, small elastic coefficients $k_{11} + k_{33}$ and k_{22} , large flexoelectric parameter $e_{11} - e_{33}$, long and constant pitch, thin layer and zero dielectric anisotropy are required.

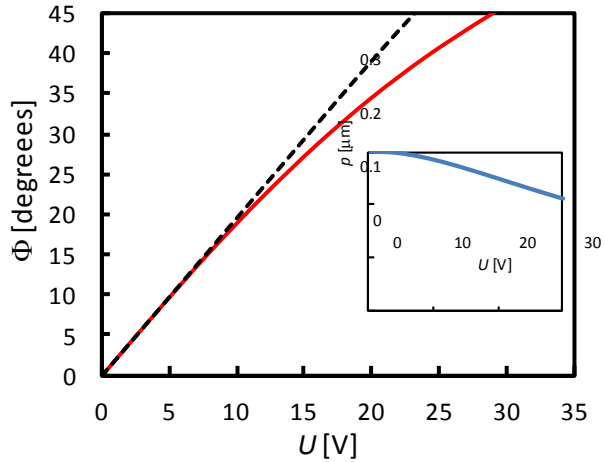


Fig. 5. Voltage dependences of the rotation angle Φ ; dashed line: pitch maintained at $p_0 = 0.3 \mu\text{m}$, full line: pitch freely varying with voltage as shown in the insert. The parameters set (a) mentioned in Table 1 is used in both cases.

REFERENCES

- [1] Patel J.S., Meyer R.B. 1987. Flexoelectric electro-optics of a cholesteric liquid crystal. *Phys. Rev. Lett.* 58: 1538-1540.
- [2] Rudquist P., Buivydas M., Komitov L., Lagerwall S.T. 1994. Linear electrooptic effect based on flexoelectricity in a cholesteric with sign change of dielectric anisotropy. *J. Appl. Phys.* 76: 7778-7783.
- [3] Rudquist P., Carlsson T., Komitov L., Lagerwall S.T. 1997. The flexoelectro-optic effect in cholesterics. *Liq. Cryst.* 22: 445-449.
- [4] Rudquist P. Lagerwall S.T. 1997. On the flexoelectric effect in nematics. *Liq. Cryst.* 23: 503-510.
- [5] Coles H.J., Morris S.M., Choi S.S., Castles F. 2010. Ultrafast switching liquid crystals for next-generation transmissive and reflective displays. *Proc. SPIE 7618. Emerging Liquid Crystal Technologies V.* 7618-14.
- [6] Lee S.D., Patel J.S., Meyer R.B. 1990. Effect of flexoelectric coupling on helix distortions in cholesteric liquid crystals. *J Appl Phys.* 67:1293-1297.
- [7] Xiuze Wang, Fells J.A.J., Welch C., Tamba M.-G., Mehl G.H., Morris S.M., Elston S.J. 2018. Characterization of large tilt angle flexoelectro-optic switching in chiral nematic liquid crystal devices. *Liq. Cryst.* 46:408-414.
- [8] Bolis S., Tartan C.C., Beeckman J., Kockaert P., Elston S.J., Morris S.M. 2018. Solvent-induced self-assembly of uniform lying helix alignment of the cholesteric liquid crystal phase for the flexoelectro-optic effect, *Liq. Cryst.* 45: 774-782.

- [9] Varanytsia A., Chien L.-C. 2015. Fast flexoelectric liquid crystal switching based on polymer-stabilized uniform lying helix. 2015. IEEE Photonics Conference (IPC). Reston, VA USA. pp. 38-44.
- [10] Xiuzhe Wang, Fells J.A.J., Yip W.C. Taimoor A., Jia-de Lin, Welch C., Mehl G.H., Booth M.J., Wilkinson T. D., Morris S.M., Elston S.J. 2019. Fast and low loss flexoelectro-optic liquid crystal phase modulator with a chiral nematic reflector. *Sci. Rep.* 9:7016.
- [11] Born M., Wolf E. *Principles of Optics* - Pergamon Press Oxford, 1964.
- [12] Derfel G, Buczkowska M. 2015. Macroscopic model formulae describing anisotropic anchoring of nematic liquid crystals on solid substrates. *Sci. Bull. Techn. Univ. Lodz, Physics.* 36: 5-12.
- [13] Babakhanova G., Parsouzi Z., Paladugu S., Wang H., Nastishin Y. A., Shiyanovskii S.V., Sprunt S., Lavrentovich O.D. 2017. Elastic and viscous properties of the nematic dimer CB7CB. *Phys. Rev. E* 96: 062704.
- [14] Morris S. M., Clarke M. J., Blatch A. E., Coles H. J. 2007. Structure-flexoelastic properties of bimesogenic liquid crystals. *Phys. Rev. E* 75: 041701.
- [15] Coles H., Clarke M., Morris S., Broughton B., Blatch A.J. 2006. Strong flexoelectric behavior in bimesogenic liquid crystals. *Appl. Phys.* 99: 34104.
- [16] Buczkowska M., Derfel G. 2017. Spatially periodic deformations in planar and twisted flexoelectric nematic layers. *Phys. Rev. E* 95: 062705-1 - 062705-8.
- [17] Corbett D.R., Elston S.J. 2011. Modelling the helical-flexo-electro-optic effect. *Phys Rev E.* 84: 041706-1 - 041706-13.
- [18] Outram B.I., Elston S.J. 2013. Dielectric enhancement of chiral flexoelectro-optic switching. *Liq. Cryst.* 40: 1529-1534.

EFEKT FLEKSOELEKTRO-OPTYCZNY O DUŻYM KĄCIE OBROTU OSI OPTYCZNEJ

Streszczenie

Symulowano numerycznie efekt fleksoelektro-optyczny w warstwach nematyków chiralnych. Obliczenia dotyczyły materiałów o krótkim skoku, z osią helisy równoległą do płaszczyzny warstwy. Symulowano odkształcenia związane z dużymi kątami obrotu osi optycznej warstwy wokół normalnej do warstwy, które pozwalają uniknąć gromadzenia się jonów na elektrodach i kontrolować efekt elektrooptyczny napięciem prostokątnym. Zbadano wpływ wybranych parametrów na skuteczność tego efektu.